

Fourier domain optical coherence tomography with an 800 μm diameter axicon lens for long-depth-range probing

Kye-Sung Lee¹, Chuck Koehler, Eric G. Johnson, and Jannick P. Rolland
College of Optics and Photonics: CREOL & FPCE, University of Central Florida,
4000 Central Florida Blvd., Orlando FL 32816

ABSTRACT

Recently, Fourier domain optical coherence tomography (FDOCT) has attracted much attention due to the significantly improved sensitivity and imaging speed compared to time domain OCT. The large depth of focus is necessary to image a long-depth-range sample with constant transverse resolution in FDOCT where dynamic focusing is not considered. Under such imaging scheme, an axicon lens can be used instead of a conventional focusing lens in the sample arm of OCT to achieve both high lateral resolution and a long depth of focus simultaneously. In this study, a 800 μm diameter axicon lens was fabricated on a silica wafer. We incorporated the fabricated axicon lens into the sample arm of our FD OCT system and investigated the lateral resolution over a long depth range, compared to the same FD OCT system using a conventional lens.

Keywords: Fourier-domain optical coherence tomography, optical coherence tomography, axicon lens

1. Introduction

Optical coherence tomography (OCT) is a highly sensitive biomedical imaging technique that enables high resolution, cross-sectional imaging in biological tissues and other turbid materials.¹ High axial resolution of OCT is realized by use of a broadband light source whereas the lateral resolution is determined by the numerical aperture of the focusing lens. Although a large numerical aperture of a conventional focusing lens in the sample arm of OCT enables high lateral resolution imaging, a small numerical aperture is required to achieve a large depth of focus that allows making a constant transverse resolution image over a long depth range. To overcome this limitation, an axicon lens was recently designed and incorporated into the sample arm of an interferometer to achieve both high lateral resolution and a large depth of focus simultaneously² and dynamic focusing lenses were used to maintain high transverse resolution over a long depth range.³

Recently, Fourier domain optical coherence tomography (FD OCT) has attracted significant interest because of its improved sensitivity and imaging speed when compared to time domain OCT (TD OCT).⁴ Axial and lateral resolutions of FD OCT are also determined by the source coherence length and the numerical aperture of the focusing lens respectively just like in TD OCT. An axicon lens can be used as a focusing lens in the sample arm of FD OCT to achieve high lateral resolution and constant intensity over long depth range of imaging because axicon lenses are optical elements that produce a long, narrow focal line along the optical axis instead of the usual focus point of a conventional lens.⁵

In Section 2, we compare theoretically the impacts of an axicon lens with that of a conventional lens to the depth of focus and the lateral resolution over the depth. In Section 3 we demonstrated the fabrication of a 800 μm diameter axicon lens and FD OCT used in the experiment. In Section 4, we showed the focusing characteristics and OCT image quality of an axicon lens and a conventional lens.

¹ kslee@creol.ucf.edu; Phone: 407-823-6853; Fax: 407-823-6880

2. Theory

A schematic of an axicon lens used in FD OCT as a focusing lens is shown in Fig. 1.

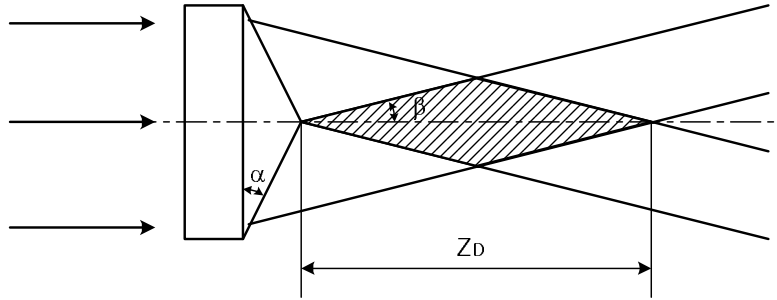


Fig 1. Schematic of an axicon lens

The depth of focus (DOF) Z_D is defined as the distance from the axicon apex to the geometrical shadow for full-facet illumination and given for small angle α of the axicon lens as

$$Z_D = \frac{d}{2(n-1)\alpha}, \quad (1)$$

where d denotes the diameter of the collimated incident beam on the axicon lens and n is the refractive index of the axicon lens. The transverse intensity distribution created by a collimated incident beam passing through an axicon lens is described by the first order Bessel function. The central lobe size of the first order Bessel is given by

$$\rho_0 = \frac{2.4048\lambda}{2\pi \sin \beta}, \quad (2)$$

where λ is the central wavelength of the incident beam and β is the beam deviation angle with respect to the optical axis of the axicon lens, shown in Fig. 1, which can be calculated as a function of the axicon angle α as

$$\beta = \sin^{-1}(n \sin \alpha) - \alpha. \quad (3)$$

The central lobe size ρ_0 is constant in the DOF Z_D because the beam deviation angle β is also constant within the geometrical shadow as shown in Fig.1. This property yields a constant lateral resolution within DOF in OCT. On the other hand, a conventional lens such as a spherical lens makes a different beam intensity profile width w according to the deviation from the nominal focus plane as shown in Fig. 2.

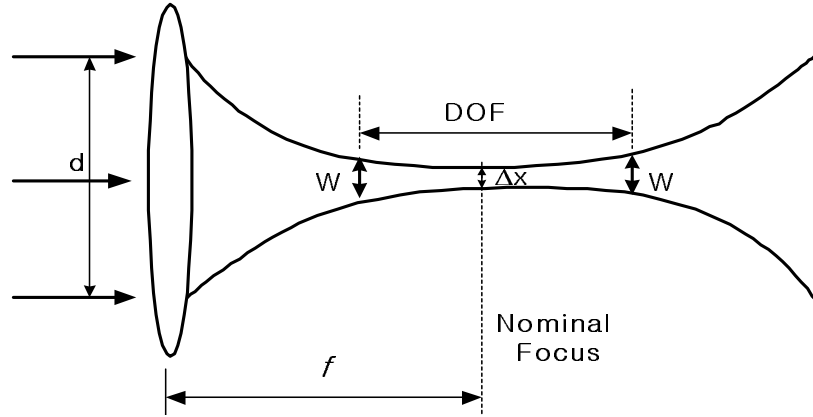


Fig.2. Schematic of a spherical lens

The full width Δx of the beam profile at a nominal focus plane by a conventional lens is given by

$$\Delta x = \frac{4\lambda}{\pi} \left(\frac{f}{d} \right) , \quad (4)$$

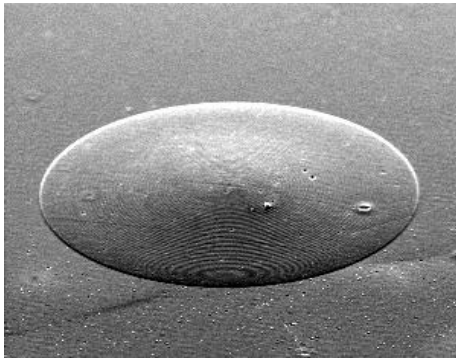
where f is the effective focal length of the conventional lens, and d is the diameter of the collimated incident beam. The DOF shown in Fig.2 can be described as Eq. (5) in case of a lens having a small numerical aperture,

$$DOF \approx \frac{2 \cdot w \cdot f}{d} . \quad (5)$$

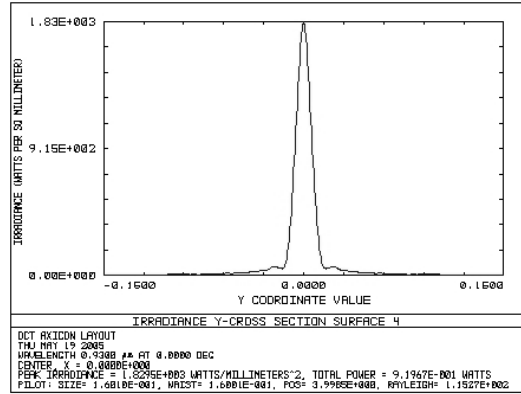
Therefore, a high lateral resolution can be achieved around a nominal focus plane by a conventional lens however the other lateral resolutions at deviated planes from the focal plane get worse due to the increased diameter of the beam.

3. Axicon Fabrication and Experiment Method

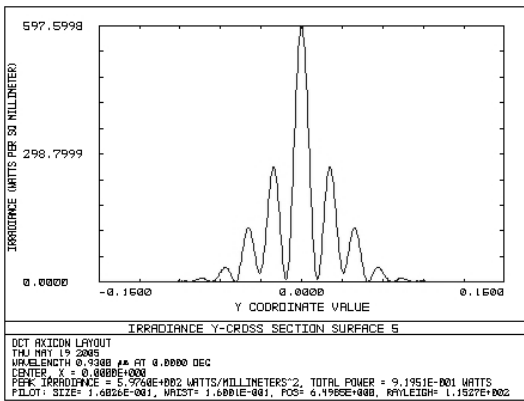
We designed and fabricated an 800 μ m diameter axicon lens on silica wafer. An axicon phase mask pattern was written into Polymethyl-methacrylate (PMMA) on an E-beam machine, and then used in a stepper as a phase mask to create an analog axicon profile on a silica wafer. It was then developed and etched into the silica wafer. The fabricated axicon picture is shown in Fig. 3 (a). We also analyzed the etched axicon pattern on the silica wafer with the Zygo interferometer to generate polynomial curve-fitting coefficients from the fabricated analog profile data. Then the curve-fitting data was placed into an optical system design software, Zemax, to perform simulations to get beam profiles shown in Fig 3 (b), (c), and (d) over the DOF. The fabricated axicon lens has about a 3 degree axicon angle and the corresponding DOF Z_D and central lobe width ρ_0 of beam profile are given by 15mm and 13 μ m with Eq. (1) and Eq. (2).



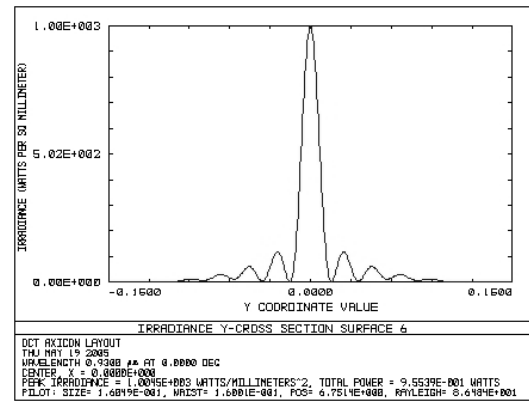
(a)



(b)



(c)



(d)

Fig.3. (a) SEM picture of the fabricated axicon, (b) Beam pattern at the start of the depth-of-focus (c) Beam pattern at the middle of the depth-of-focus (d) Beam pattern at the end of the depth-of-focus

The fabricated axicon lens was incorporated into the sample arm of a Fourier domain OCT to test its performance. The schematic diagram of the system is shown in Figure 4. The FD-OCT system consists of a broad bandwidth (120nm at full-width-at-half-maximum centered at 800nm) Titanium:Sapphire laser and a commercial spectrometer with a CCD array and a 80/20 fiber coupler which makes two arms of the interferometer. The 80% beam from the coupler is collimated and then incident on the axicon lens. So the light is focused on the sample after propagating through the lens. The other 20% beam is reflected by a mirror through the Fourier domain optical delay line in the reference arm whose main function is to control the overall dispersion in the system.⁶

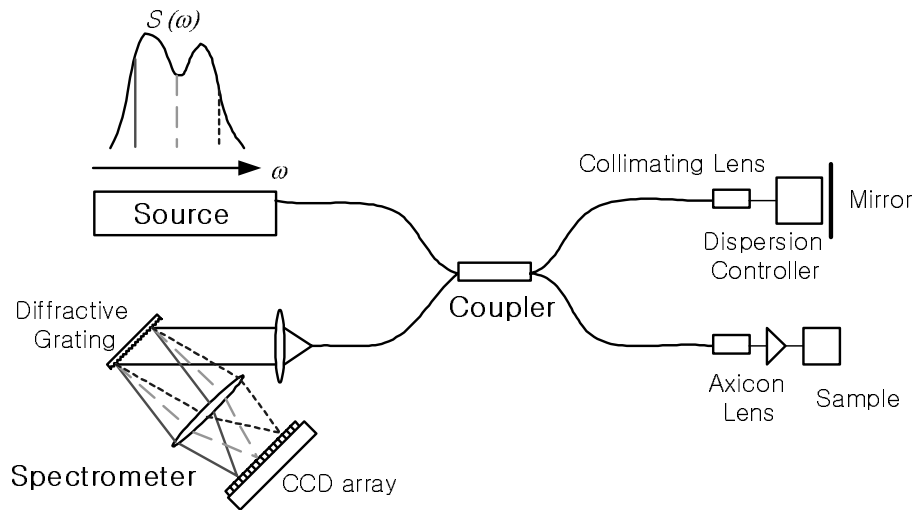


Fig. 4. Schematic diagram of a Fourier-domain OCT with an axicon as a focusing lens in the sample arm.

4. Results

We first measured the intensity profile of the collimated beam before the focusing lens as shown in Fig. 5 and then measured the beam profile after passing through either the axicon lens or the spherical lens as a function of the distance from the lens. The collimated beam diameter was around $800\mu\text{m}$ and its profile was shaped as a Gaussian as shown in Fig. 5.

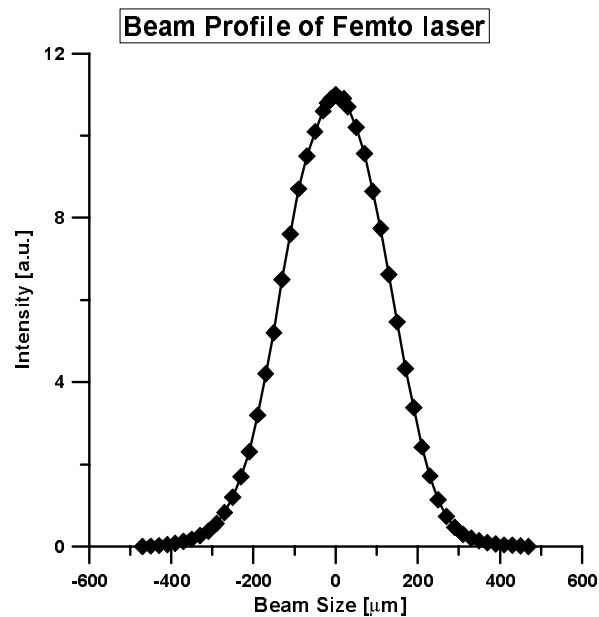


Fig. 5. Intensity profile of the collimated beam before the axicon lens.

The collimated beam was incident on a $800\mu\text{m}$ diameter axicon lens and the beam profiles at different planes from the axicon apex were measured as shown in Fig. 6 (a). The geometrical depth of focus Z_D was almost 15mm which was

estimated in section 3, and the central lobe widths were constant of value $13\mu\text{m}$ over the depth of focus. The peak intensity was decreased as the measured plane is moved away from the axicon lens because the incident beam is Gaussian in shape. For comparison with a conventional lens we also measured the beam profiles at different distances from the focal planes of a 8mm focal length spherical lens as shown in Fig. 6 (b). The full width Δx of the beam profile at the nominal focus plane by the spherical lens was computed to be $10\mu\text{m}$ with Eq. (4). Although the beam width was better than that of the axicon lens at the focal plane, the beam width at 2mm away from the focal plane was found to be around $200\mu\text{m}$ based on Eq. (5) which is highly broadened compared to that of the axicon lens.

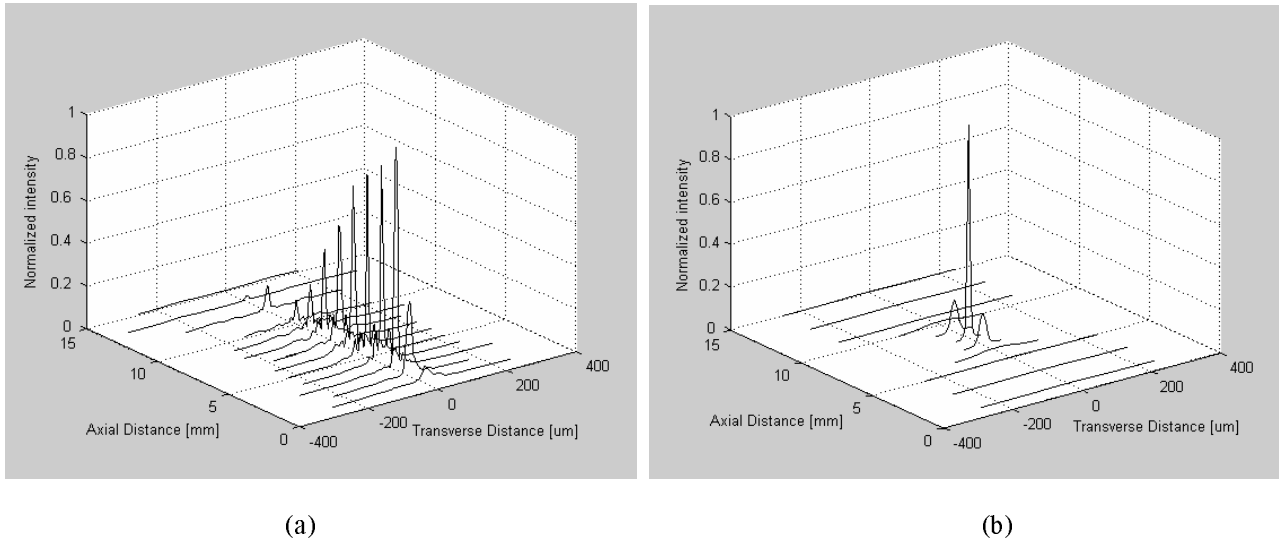


Fig. 6. Beam intensity profile after (a) an axicon lens (b) a spherical lens according to the distance from the lens

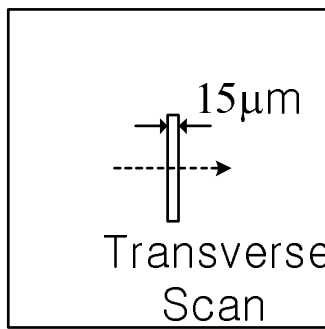
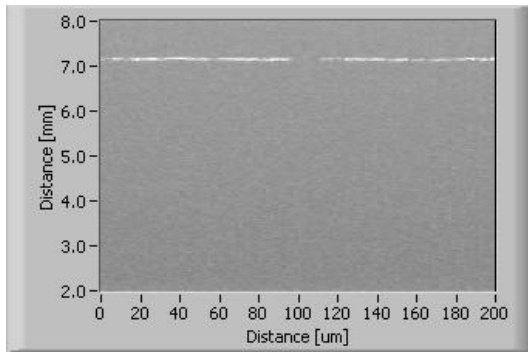
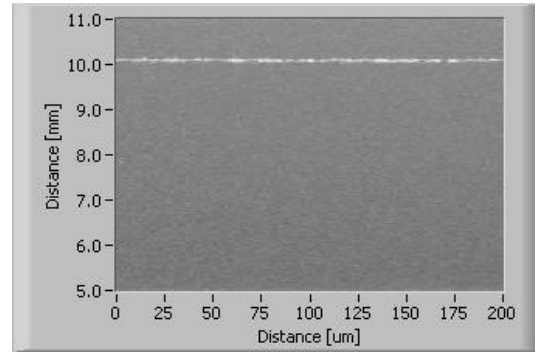


Fig. 7. A $15\mu\text{m}$ slit

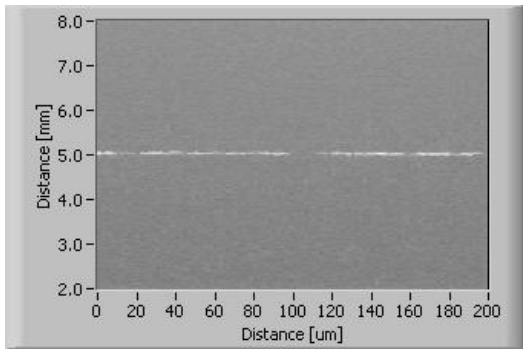
We imaged a $15\mu\text{m}$ slit shown in Fig 7 at three different distances from the lens for both an axicon lens and a spherical lens. Fig. 8 (a), (c), (e) are the OCT images of the slit at the distances of 7mm, 5mm, and 3mm away from an axicon lens. Fig. 8 (b), (d), (f) are the OCT images of the slit at the distances of 10mm, 8mm, and 6mm away from a spherical lens. The $15\mu\text{m}$ slit was imaged at 7mm, 5mm, and 3mm as shown in Fig. 8 (a), (c), (e) while the spherical lens has an ability to image it only at focal plane as shown in Fig. 8 (d). Results show good correlation between the sharpness of the point spread function and the ability to resolve the slit hole clearly observed in Figs. 8(a), (c), (d), and (e).



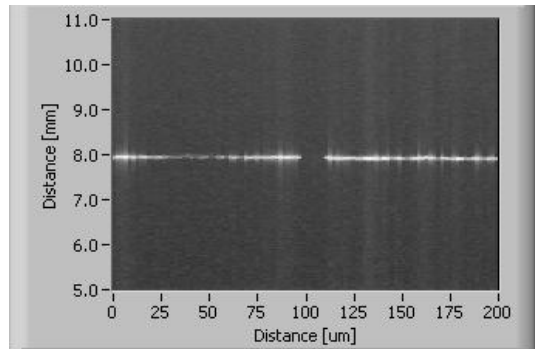
(a)



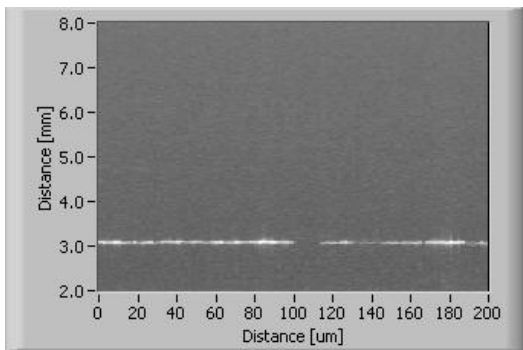
(b)



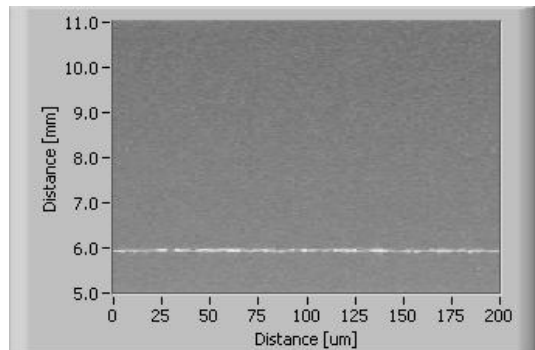
(c)



(d)



(e)



(f)

Fig.8. OCT images of a 15 μ m slit transversally scanned at distances of (a) 7mm, (c) 5mm, and (e) 3mm away from an axicon lens and (b) 10mm, (d) 8mm, and (f) 6mm away from a spherical lens

5. Conclusion and Discussion

In this paper, we demonstrated the impact of an axicon lens on the lateral resolution in OCT compared to a conventional lens. An axicon lens incorporated in OCT can render a constant high lateral resolution over long depths of focus

compared with the conventional lens which can image only short depth ranges with high lateral resolution. We showed in the paper the superior ability of the system with an axicon to resolve a 15 μ m slit across a 4mm DOF compared to a spherical lens. However higher signal to noise ratio images can be obtained around the focal plane of a spherical lens in OCT because the full beam power is sent to a small area around the focal point while the OCT adapted with an axicon lens yields much of the power being distributed over a long depth of focus. Thus an axicon lens coupled with higher power source can yield both superior resolution and good signal to noise ratio.

Acknowledgements

This research was supported in part by the Florida Photonics Center of Excellence, the NSF IGERT program, the UCF Presidential Instrumentation Initiative, and the DARPA & NSF PTAP program.

References

1. D. Huang, E. A. Swanson, C. P. Lin, J. S. Schuman, W. G. Stinson, W. Chang, M. R. Hee, T. Flotte, K. Gregory, C. A. Pulifito, and J. G. Fujimoto, "Optical coherence tomography," *Science* 254, 1178-1181 (1991).
2. Zhihua Ding, Hongwu Ren, Yonghua Zhao, J. Stuart Nelson, and Zhongping Chen, "High-resolution optical coherence tomography over a large depth range with an axicon lens," *Optics Letters* 27, 243-245 (2002).
3. W. Drexler, U. Morgner, F. X. Kortner, C. Pitris, S. S. Boppart, X. D. Li, E. P. Ippen, and J. G. Fujimoto, "In vivo ultrahigh-resolution optical coherence tomography," *Optics Letters* 24, 1221-1223 (1999).
4. R. Leitgeb, C. K. Hitzenberger, and A. F. Fercher, "Performance of fourier domain vs. time domain optical coherence tomography," *Optics Express* 11, 889-894 (2003), <http://www.opticsexpress.org>.
5. Anna Burvall, Katarzyna Kolacz, Zbigniew Jaroszewicz, and Ari T. Friberg, "Simple lens axicon," *Applied Optics* 43, 4838-4844 (2004).
6. Kye-Sung Lee, A. Ceyhan Akcay, Tony Delemos, Eric Clarkson, and Jannick P. Rolland, "Dispersion control with a Fourier-domain optical delay line in a fiber-optic imaging interferometer," *Appl. Opt.* 44, 4009-4022 (2005).